A Modular Textile Antenna Design using Snap-on Buttons for Wearable Applications

Shengjian Jammy Chen, *Student Member, IEEE,* Thomas Kaufmann, *Member, IEEE,*
Damith Chinthana Ranasinghe, *Member, IEEE,* and Christophe Fumeaux, *Senior Member, IEEE*

***Abstract*—An antenna design concept with detachable radiation elements offering modular geometry reconfigurabilities for wearable applications is presented. By utilizing snap-on buttons both as the radio frequency (RF) connection and mechanical holding mechanism, different modularly interchangeable microstrip patches are employed to demonstrate geometry reconfigurabilities in terms of polarization and resonance frequency. The uniqueness of the design arises from the fact that all configurations share one common feed structure which consists of a two-layered substrate including snap-on buttons, a ground plane and a proximity coupled feed. To show the concept, modular realizations with different functionalities in terms of polarization or resonance frequency are demonstrated in this paper. Firstly, a detachable patch offering interchangeable right hand circular polarization (RHCP) and left hand circular polarization (LHCP) at 5 GHz is proposed. Secondly, a demonstration of a planar inverted-F antenna (PIFA) concept offering interchangeable resonance frequencies for the 2.4- and 5.3-GHz bands of wireless local area networks (WLAN) is given. Finally a patch module designed for 8 GHz operation is presented to show the versatility in frequency modularity. Experimental results of the fabricated antennas in free-space, worn by a torso phantom and in bending conditions, validate the concept and prove that this type of modular design offers convenient, passive, low cost and versatile system reconfigurabilities which can benefit wearable applications.**

***Index Terms*—Modular antennas, wearable antennas, textile antennas, snap-on button.**

I. Introduction

In recent years, flexible and wearable antenna designs have received significant attention due to the dramatically increasing demands in various wearable electronic systems [1], [2]. Applications include mobile communications, wireless medical monitoring/diagnosing and military applications [3], [4]. Besides conventional antenna requirements, wearable antennas are expected to be flexible, lightweight, low-cost and garment-integratable [5], [6]. As a result, conductive textiles have been emerging as one of the most promising conducting materials [7], [8]. Many wearable devices made from conductive textiles such as patch antennas [9]–[11] and arrays [12], ultra-wideband [13], [14] and ultra-wideband-notched [15] antennas, as well as antennas based on fundamental mode [16] and half-mode [17], [18] substrate-integrated waveguides have been reported. Moreover, clothing closure accessories have been exploited as support for antenna design. For example, metallic buttons for textiles have been designed as wearable antennas [19], [20], and commercial metallic snap-on buttons also have been proposed as a practical and economical radio frequency (RF) connection solution for wearable systems, since they can form detachable RF connection with suitable RF performance [21]–[23]. This leads to the idea of making specific radiation elements detachable with snap-on buttons to achieve modular antenna designs, thus enabling passive reconfigurability of the overall system. Although this requires manual operation, passive reconfiguration promotes ease of antenna design [24] and versatile wearable antenna integration since no active components and bias circuits are needed.

Modular antenna designs have been proposed in various wireless communication systems such as mobile phones [25], cellular communication base-stations [26] and avionics systems [27]. They can be categorized into two main groups according to their modular antenna elements, namely identical and different modular antenna elements. Typically, identical modular antenna elements are employed as building blocks for antenna array designs [26], [28]. With such modular designs, the array dimensions can be easily reconfigured. On the other hand, modular designs with different antenna modules can be found in systems featuring interchangeable antennas which share one common feed design [25], [27], [29]. These antenna modules are usually of same outline geometry to satisfy the requirements of same fitting and feeding, even if they are serving different functionalities. Such modular antenna designs bring valuable advantages including low manufacturing cost, easy maintenance and most importantly passive system reconfigurability.

In this paper, a modular antenna design based on metallized fabric and flexible low-permittivity foam substrate is presented for wearable applications, providing possible system reconfigurabilities for polarization and resonance frequency. Commercial snap-on buttons are employed as RF connectors and mechanical fixtures to enable easy detachability of the modular antenna radiating elements. Various types of antenna functions can be conveniently achieved by flipping-over, interchanging or ground-shorting the patch modules. To demonstrate the concept, three patch modules offering interchangeable circular polarizations and resonance frequencies for 5 GHz, WLAN 2.4-GHz, 5.3-GHz (IEEE 802.11) bands and 8 GHz in the X-band have been designed, realized and tested. These frequencies are chosen as representative examples, but the

Manuscript received June xx, 20xx; revised September xx, 20xx.

S.J. Chen, T. Kaufmann and C. Fumeaux are with the School of Electrical and Electronic Engineering, The University of Adelaide, Adelaide 5005, South Australia, Australia

D.C. Ranasinghe is with The Auto-ID Lab, The School of Computer Science, The University of Adelaide, Adelaide 5005, South Australia, Australia

The authors acknowledge the support of the Australian Research Council (ARC) under Discovery Projects DP120100661.

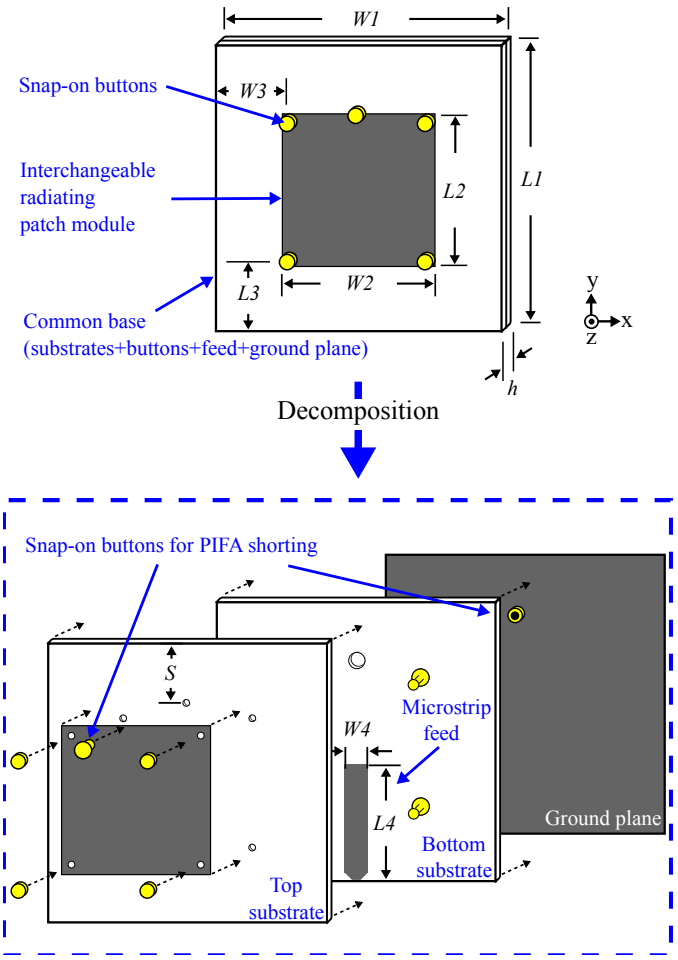

Figure 1. The proposed modular antenna and its configuration. The antenna includes a common antenna base and an interchangeable patch module designed for a specific functionality. The patch module is mounted on a common base which consists of a ground plane, two layers of substrates, an open-end microstrip proximity coupled feed and five snap-on buttons. Four snap-on buttons are used as mechanical fixtures for the various patch modules, whereas the fifth optional button is utilized as RF connector to create a short in a PIFA configuration. Various functionalities are fulfilled with dedicated patch modules.

functionality of the principle is not limited to these particular bands. The first module can offer interchangeable LHCP and RHCP at 5 GHz whereas the second one can be used in two configurations to have different resonance frequencies including 2.45 and 5.3 GHz. The third one only operates at 8 GHz with linear polarization, however, it shows a higher degree of design adaptability to illustrate nearly unlimited choices of radiation element geometry. The very good agreement between simulation and experimental results in free-space, worn by a torso phantom and in bending conditions confirm that such passive modular antenna designs can provide a low-cost, easy-maintenance solution to enable versatile system reconfigurabilities for wearable applications.

II. The Antenna Design

The generic antenna configuration is depicted in Fig. 1 and the most relevant dimensions are listed in Table I. The antenna configuration is a planar structure and it consists of an

Table I
Dimensions of the common antenna base and the outlined dimensions of the radiating patch modules.

Parameters	$W1$	$W2$	$W3$	$W4$	S
Value (mm)	40	19.5	13	6.5	10.5
Parameters	$L1$	$L2$	$L3$	$L4$	h
Value (mm)	40	18.5	13.5	15	3.2

interchangeable modular radiating patch dedicated to a specific application and a common base which includes a microstrip proximity coupled feed, a two-layered substrate and five commercial snap-on button connectors. In this paper, 5 GHz, WLAN 2.4- and 5.3-GHz (IEEE 802.11) bands as well as 8 GHz in the X-band have been chosen as the designed antenna operation frequencies for illustration. But it is emphasized that the concept is not limited to these frequencies.

A. Antenna Structure and Material

To obtain flexibility without sacrificing conductivity, the radiating patch elements, the microstrip feed and the ground plane are made from a silver-coated nylon RIPSTOP fabric (commonly denoted as silver fabric) with a dc sheet resistance of 0.01 $\Omega/\square$ and a thickness of approximately 100 μm. The various patches can be fixed on top of the common base with four pairs of engaged snap-on buttons which provides detachability and consequently interchangeability. For the same reason, a proximity-coupled feed is adopted for the generic design since the physical separation between feed and radiating element permits a free-standing detachable patch. The substrate contains two layers of 1.6-mm-thick highly flexible Cuming Microwave C-Foam PF-4 foams with relative permittivity $\varepsilon_r = 1.06$ and loss tangent $\tan\delta = 0.0001$. This two-layer structure serves two functionalities including antenna elements separation and strict immobilization of snap-on buttons. An open-ended microstrip line serving as the antenna feed and four male snap-on buttons serving as the patch fixtures are embedded between the top- and bottom-layer substrate. Note that the top-layer substrate is cut with four holes for the snap-on button male pin to go through. A fifth female snap-on button placed to provide a shorting post for a proposed planar inverted-F antenna (PIFA) configuration is sewed onto the ground plane using conductive threads and thus a hole is individually trimmed through both substrate layers to accommodate it.

B. Snap-on Buttons

The snap-on buttons are the key components which mechanically and electrically enable low-cost and practical detachability and interchangeability for the patch modules. The chosen commercial snap-on buttons and their main dimensions are both included in Fig. 2. On the one hand, they are selected as mechanical fixtures since their size are appropriate for the patch modules, and more importantly, they offer solid mechanical performance. A dedicated test done in [23] indicates that

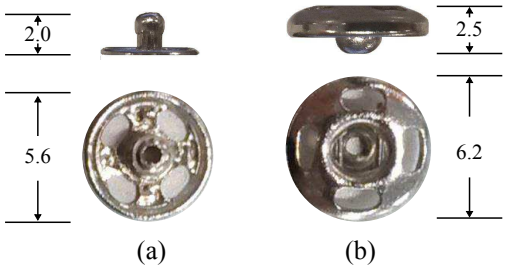

Figure 2. Snap-on buttons and their dimensions (mm). (a) Male snap-on button. (b) Female snap-on button.

an approximate 3 N force is needed to undo engaged buttons of this type. On the other hand, since these snap-on buttons offer detachable connection with satisfactory RF performance at least up to 5 GHz [23], they are also chosen as an RF connector for the PIFA antenna configuration.

C. Patch Modules

Since the radiation element is detachable and interchangeable, different patch modules can be designed to serve various functionalities. Moreover, this feature can benefit a low maintenance cost since easy servicing and economical repair can be achieved by direct component replacement. For illustration purpose, three different types of patch modules are designed to achieve five interchangeable functionalities in terms of polarization and resonance frequency respectively. The first two modules are single-layer structures and can serve two functionalities individually: As shown in Fig. 3-(a), the first patch module aims at providing RHCP or LHCP at 5 GHz, depending on the orientation of the diagonal slot. The second patch module shown in Fig. 3-(b) can resonate either at 2.45 or 5.3 GHz which is controlled by its orientation and the engagement of a shorting button to create a PIFA operation (Fig. 1). In contrast, the third patch module only provides a single functionality but with a higher degree of freedom in terms of module design: An illustrative example is designed for operation at 8 GHz and requires a two-layered structure, as shown in Fig. 3-(c). This last arrangement structure offers more freedom in module design, however at the cost of additional complexity.

The alignment and the attaching/detaching repeatability of these patch modules are critical for the antenna performance and thus particular attention is required with regard to the module design. Firstly, the silver fabric is chosen for the module materials as it is conductive, flexible and, more importantly in this case, robust enough to remain undistorted for numerous interchange of modules. Secondly, four positioning holes are created in the modular patches to ensure an accurate module alignment with the male buttons embedded in the top substrate layer. These holes are precisely cut using a laser milling machine. To tightly confine the module alignment with the button fixtures, the hole radius is determined to be 0.7 mm which corresponds to the exact dimension of the neck of the male pin. Very stable alignment and attaching/detaching repeatability have been observed during the measurement campaign for the most-frequently-used modules.

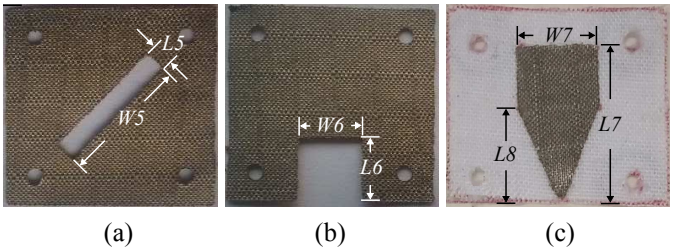

Figure 3. Patch modules and their dimensions. (a) Patch module designed for 5 GHz RHCP/LHCP, made from silver fabric. (b) Patch module designed for 2.45/5.3 GHz, made from silver fabric. (c) Patch module designed for 8 GHz, including a cotton fabric substrate and a silver fabric patch.

Table II
DIMENSIONS OF THE PATCH MODULES SHOWN IN FIG. 3.

Parameters	$W5$	$W6$	$W7$	
Value (mm)	12	6	7.5	
Parameters	$L5$	$L6$	$L7$	$L8$
Value (mm)	2	6	15.2	9.3

The outlined geometry and the other dimensions of these patches can be found in Table I and II, respectively. All simulations are performed with CST Microwave Studio 2014 (CST). The design process starts with the circularly polarized patch modules, since matching to the feeding structure is the most challenging to achieve compared to the other modules.

1) Patch module for 5-GHz orthogonal circular polarization: Initially, as expected for a rectangular microstrip antenna design on unit permittivity substrate, the patch dimensions are set to be a half of the wavelength at the chosen operating frequency. The patch is then tuned to obtain approximately a 5% higher resonance frequency which will compensate the influence from the diagonal slot introduced later. To achieve circular polarization, the method using a diagonal slot perturbation is selected and initial dimensions of the slot are determined using formula (8.20) given in [30]

$$\left|\frac{\triangle A}{A}\right| = \frac{1}{2Q_0}. \tag{1}$$

This formula is utilized to find out the initial slot dimensions, where $\triangle A$ is the slot area ($L5 \times W5$), A is patch area ($L2 \times W2$) and Q_0 is the antenna unloaded quality factor. The value of Q_0 is estimated through the fractional bandwidth ($\triangle f/f_0$) and the voltage standing wave ratio (VSWR) obtained from simulation results using the relationship [31]

$$\frac{\triangle f}{f_0} = \frac{\text{VSWR-1}}{Q_0\sqrt{\text{VSWR}}}. \tag{2}$$

Consequently the only unknown $\triangle A$ can be determined accordingly as a starting value. An optimal slot dimension combination which yields a nearly 0-dB axial ratio (AR) is then gained through parameter sweeps in CST. Because of the introduction of the diagonal slot, the resonance frequency is now lower and consequently closer to 5 GHz. Subsequent tuning of $L1$ and $W1$ is required to achieve a maximum

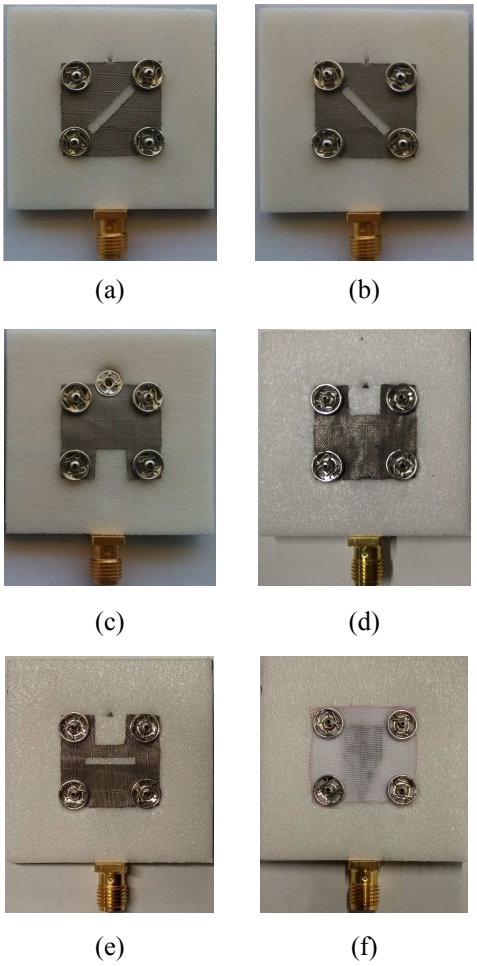

Figure 4. Antenna realizations. (a) Antenna loaded with circularly polarized patch module in RHCP configuration. (b) Antenna loaded circularly polarized patch module in LHCP configuration. (c) Antenna loaded with linear patch module in PIFA configuration (2.45 GHz). (d) Antenna loaded with linear patch module in normal configuration (5.3 GHz). (e) Antenna loaded with linear patch module with slot in normal configuration. (f) Antenna loaded with 8-GHz patch module.

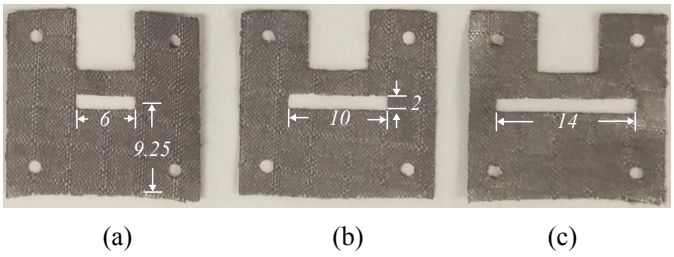

Figure 5. 5.3 GHz Patch modules with transverse slots of different lengths but with the same width of 2 mm. (a) Patch module with a 6-mm long slot. (b) Patch module with a 10-mm long slot. (c) Patch module with a 14-mm long slot.

impedance bandwidth and an AR below 1 dB, both centered at 5 GHz. Finally the length of the open microstrip feed is adjusted for best impedance matching. It is worth mentioning that since the microstrip feed line is fixed from this point on, matching techniques for all subsequently designed patch modules will require extra effort. The antenna loaded with the designed patch, as shown in Fig. 4-(a), provides RHCP while in contrast the one shown in Fig. 4-(b) provides LHCP. The circular polarization is easily interchangeable by flipping the patch accordingly.

2) Patch module for 2.45- and 5-GHz WLAN operation: As illustrated in Fig. 1 and Fig. 4-(c), a fifth female snap-on button sewed onto the ground plane can be engaged to a male counterpart to form a patch-to-ground electrical shorting. As a consequence, the antenna operates then as a PIFA antenna (quarter-wavelength patch), as shown in Fig. 4-(c), instead of the standard half-wave microstrip patch configuration as shown in Fig. 4-(d). The two resonance frequencies are generally both inversely proportional to the patch length $L2$ and the lower resonance frequency (PIFA) is also additionally dependent on the shorting button's vertical position S. It is worth to mention that once the circular module design is completed, the outline ($L2$ and $W2$) is determined for all other patch modules which are made of a single layer structure, in contrast to the two-layered 8-GHz module. Therefore, S is utilized to tune the lower resonance frequency. Furthermore, transverse slots can be introduced within the patch to individually adjust the higher resonance frequency. Since the resonance frequency tunability is important for obtaining various system reconfigurability, three of this module variations with different transverse slots have been fabricated and tested to verify the prediction. As displayed in Fig. 5, a 2-mm wide slot with different length of 6, 10 and 14 mm was introduced in three identical modules respectively.

As mentioned previously, the microstrip feed has been optimized for the circularly-polarized patch and thus cannot be changed. Therefore, matching technique needs to be applied to the patch modules in this case. To match the antenna in PIFA configuration, a rectangular notch with dimensions $L6 \times W6$ is required, as shown in Fig. 3-(b). This notch reduces the capacitance between the patch and the microstrip feed and hence compensates the capacitance decrease in the patch input impedance due to the ground shorting. For the half-wave configuration, a satisfactory matching is achieved by a rotation of the patch module bringing the edge without notch down, and thus leading to a similar input impedance as the circularly polarized module. The antenna in quarter-wave and half-wave configurations are illustrated in Fig. 4-(c) and (d) individually. Switching between two resonance frequencies, 2.45 GHz and 5.3 GHz, is accomplished via a simple rotation of the patch and engaging (or disengaging) the shorting snap-on button. In addition, the antenna loaded with the half-wave patch with a transverse slot of length of 10 mm is shown in Fig. 4-(e).

3) Patch module for 8-GHz X-band operation: This module consists of one layer of non-conductive fabric as a support with

the same outline geometry as the other patches and one layer of silver fabric as a radiation element resonating at 8 GHz. This two-layered arrangement provides a more adaptable way for patch module design since the radiating element has more freedom in terms of size and shape selection, while the non-conductive fabric ensures mechanical fixture. The supporting fabric was chosen as cotton textile commonly used for embroidery. The fabric has a measured thickness of approximately 200 μm, as well as a relative permittivity $\varepsilon_r = 2$ and a loss tangent $\tan\delta = 0.01$ both estimated based on fitted simulation results, which broadly agree with the measured values for cotton textiles in [32], [33].

As anticipated, the vertical length $L7$ of the radiating element is inversely proportional to the resonance frequency. The bottom of the radiating element is tapered as a triangle to get a satisfactory matching. The antenna loaded with this patch is illustrated in Fig. 4-(f). Owing to the vicinity to the radiating element, coupling to the snap-on buttons should be taken into account in the design. This can be done with simulation tools and complicated current distributions have been observed in simulated results. Moreover, the radiating patch is facing down towards to the substrate to avoid galvanic contact with the two closest female buttons.

4) Other possible functionalities: With a two-layer structure like the 8-GHz patch module, more functionalities can be fulfilled. For instance, an array of small patches can be possibly designed using this type of structure. Other patch module designs offering multiple-band or wide-band performance as well as switchable skewed beam directions can be designed through additions of slots and snap-on shorting posts. Various such further possibilities have been explored through simulations, but have not been validated experimentally and thus are not presented here for the sake of brevity. The possibilities of this modular antenna design are wide ranging in terms of variety of achievable antenna characteristics.

III. Experimental Results

For validation of the modular concept, the proposed antenna designs have been fabricated and experimentally characterized. Since the devices are designed for wearable applications, the impacts of human body proximity and bending have been investigated as well. In particular, the antenna loaded with the 5-GHz LHCP patch was utilized for a bending study as well as for the characterization on a human torso phantom, as this design is the most sensitive to tolerances.

To achieve accurate patterning of the geometry, the patch modules and microstrip feed are cut with a laser milling machine (LPKF: Protolaser S). A dedicated fixture is used to trim holes in the substrates and align the feed line and snap-on buttons onto the bottom substrate. Machine-washable fabric glue, Wash N Wear Glue White from Helmar®, is applied to attach the ground plane to the substrate, the microstrip feed/buttons to the bottom substrate, the top substrate to the bottom substrate, and the radiation patch to its fabric substrate. As only a very thin layer of the glue is required to form a permanent and solid bond, its influence on the antenna performance is deemed negligible and can be best taken into account as a slight increase in the conductor loss of the metalized textile. Conductive epoxy is adopted to mechanically and electrically connect a SMA connector to the microstrip feed. The conductive epoxy applied is the CW2400 from CircuitWorks® which offers high strength bond and excellent electrical connection with a very low volume resistivity of 0.1 $\Omega \cdot m$.

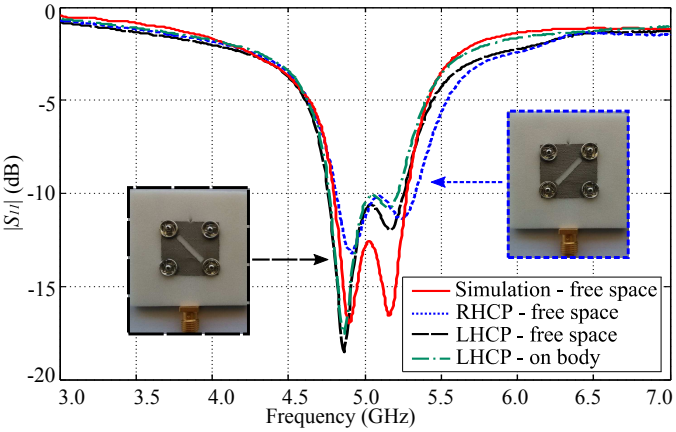

Figure 6. Reflection coefficient comparison of the antenna loaded with the circularly-polarized patch module.

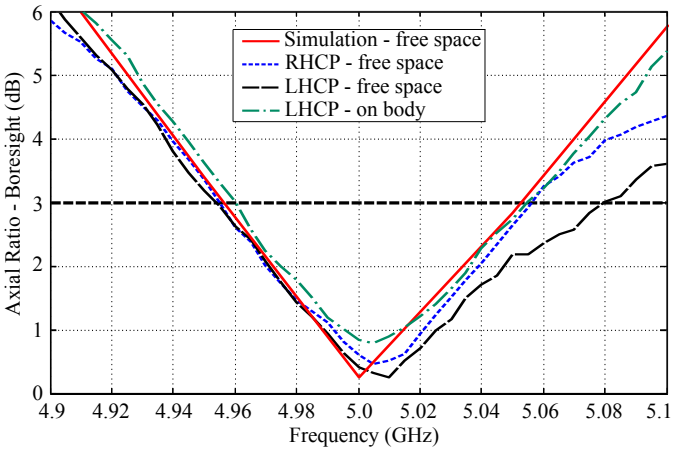

Figure 7. Boresight axial ratio of the antenna loaded with circularly-polarized patch module.

A. Antenna loaded with circularly-polarized patch module

As illustrated in Fig. 6, the measured reflection coefficients for the antenna loaded with the circularly polarized modules show a reasonable agreement with the simulated values. The measured $|S_{11}|$ parameter of the antenna yields a -10-dB impedance bandwidth from 4.75 to 5.25 GHz for the LHCP configuration and from 4.80 to 5.35 GHz for the RHCP one, which covers the target center frequency of 5 GHz. The difference is indicative of fabrication tolerances.

The simulated and measured boresight axial ratios of the antenna in free space are compared in Fig. 7 and they exhibit a very good agreement. The 3-dB axial-ratio bandwidth is from 4.95 to 5.08 GHz for the LHCP configuration and from 4.95 to

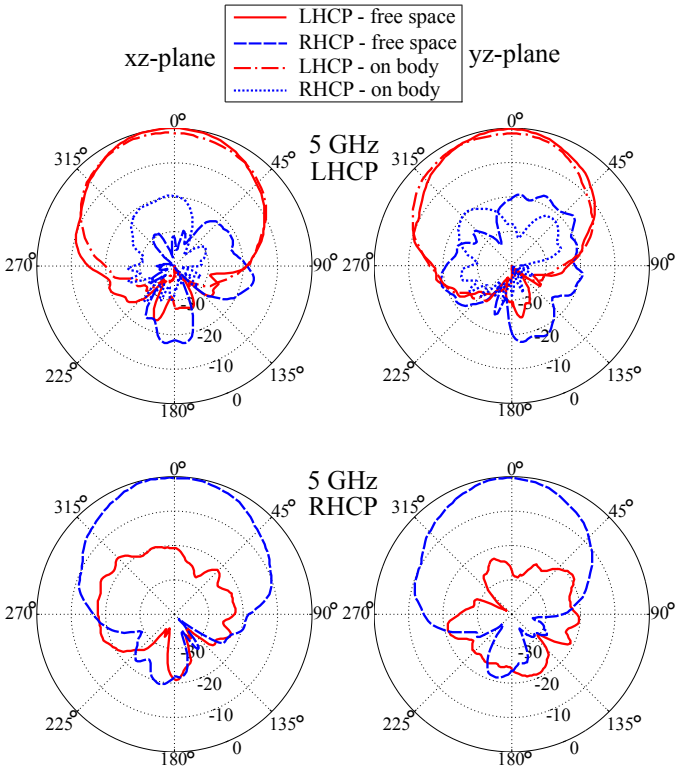

Figure 8. Measured radiation patterns of the antenna loaded with circularly-polarized patch module. The LHCP antenna patterns have been measured as well on a human torso phantom and the patterns are normalized to the results measured in free space.

5.06 GHz for the RHCP one, both centered at approximately 5.01 GHz. The whole 3-dB axial bandwidth (of 2.2%) is covered by the -10-dB impedance bandwidth (of 10%), which indicates that circular polarization is achieved as designed.

The normalized radiation patterns in xz-plane (H-plane) and yz-plane (E-plane) have been obtained through measurement in an anechoic chamber. The radiation patterns of the LHCP and RHCP antennas in free space are shown in Fig. 8. For the LHCP antenna, the desired left-handed polarization (co-polarization) has an approximately 20-dB power higher level over the unwanted right-handed polarization (cross-polarization). Due to symmetry, similar radiation patterns are obtained for the RHCP antenna configuration, but with a predominant right-handed polarization rather than the left-handed one. As anticipated for a microstrip patch antenna, all these patterns exhibit a main lobe directed in positive z direction with some small back lobes with amplitude dependent on ground plane size. In addition, a realized gain of 8.0 dBic has been measured for the LHCP antenna and this result is very close to the simulated value of 8.1 dBic.

B. Antenna loaded with patch module for WLAN

The measured $|S_{11}|$ parameters of the antenna loaded with linearly polarized patches are largely in accord with simulations, as depicted in Fig. 9. The antenna with PIFA configuration has an impedance bandwidth of around 100 MHz centred at 2.45 GHz. The half-wave patch resonates at

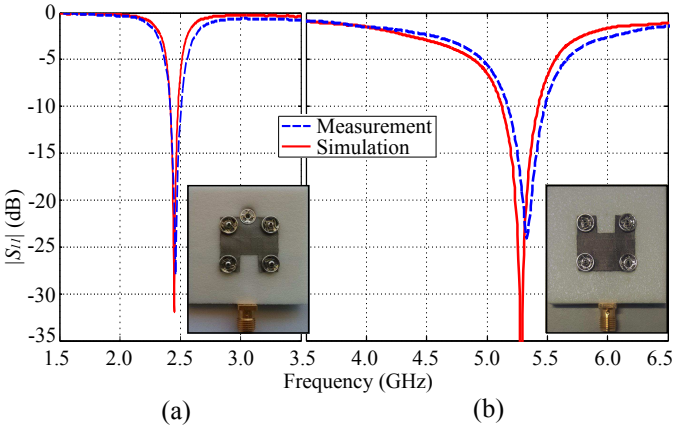

Figure 9. S-parameter comparison of the antenna loaded with linear-polarized patch module. (a) Antenna loaded with the patch module in PIFA configuration (2.45 GHz). (b) Antenna loaded with the patch module in normal configuration (5.3 GHz).

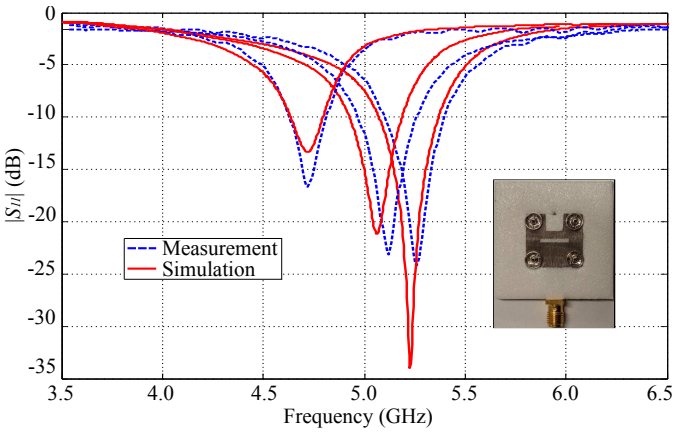

Figure 10. S-parameter comparison of the antenna loaded with slot patch modules. The lowest, medium and highest resonance frequencies correspond to the modules with slot length of 14 mm, 10 mm and 6 mm respectively.

5.33 GHz with an impedance bandwidth extending from 5.18 to 5.48 GHz.

Now considering the half-wave patches with an added transverse slot, their measured and simulated reflection coefficients are displayed in Fig. 10, showing reasonable agreement. As expected, the patch with the longest slot (14 mm) yields the lowest resonance frequency at 4.72 GHz while the highest resonance frequency 5.26 GHz is held by the one with the shortest slot (6 mm). The resonance frequency in the middle corresponds to the patch with a slot of length of 10 mm. Theoretically the resonance frequency can be further decreased by extending the slot length or introducing more slots [30].

The measured normalized radiation patterns are shown in Fig. 11. The patterns of the standard half-wave patch are as expected for this type of antenna, whereas the patterns of the quarter-wave patch show a degradation typical for PIFA antennas, with less directivity and increased cross-polarization. The measured antenna gain for the half-wave and quarter-wave patches are 7.8 dBi and 3.1 dBi, respectively. These values are close to the simulated results of 8.3 and 3.5 dBi.

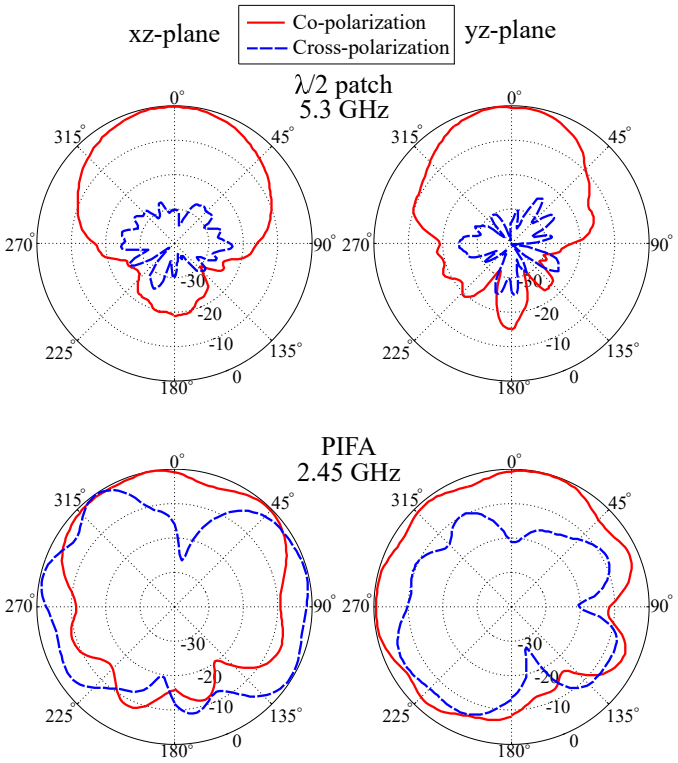

Figure 11. Measured radiation patterns of the antenna loaded with linearly-polarized 2.45- and 5.3-GHz patch modules.

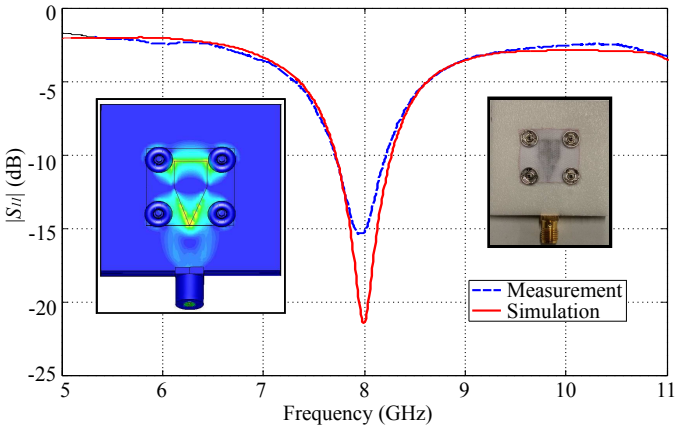

Figure 12. Measured and simulated S-parameter comparison of the antenna loaded with an 8-GHz patch module. The insets show the antenna module (right) and the simulated electric field distribution (left).

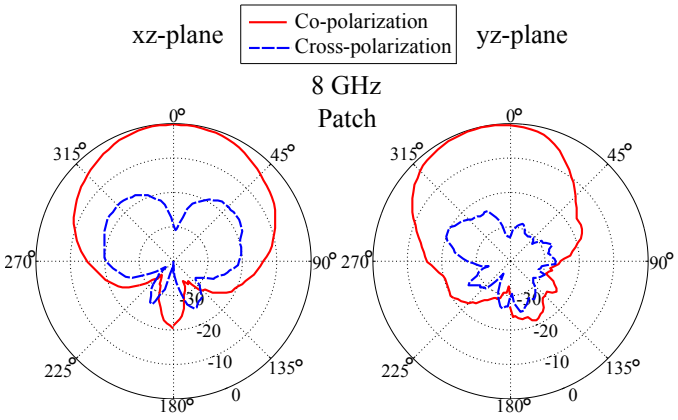

Figure 13. Measured radiation patterns of the antenna loaded with an 8-GHz patch module.

C. Antenna loaded with patch for X-band

In contrast to the previous modules, this configuration only serves one functionality, however, it illustrates a higher degree of flexibility and an implementation at a higher operation band. The measured and simulated reflection coefficients have a good correspondence, as demonstrated in Fig. 12. The antenna resonates at 8 GHz with a bandwidth of approximately 500 MHz. The measured normalized radiation patterns are portrayed in Fig 13, and as expected, standard half-wave patch radiation patterns are observed, which is confirmed by the simulated electric field distribution of the antenna shown in the inset of Fig. 12. The measured antenna gain is approximately 8.9 dBi whereas the simulated one is 9.2 dBi.

D. Human Body Impact

As an important aspect of wearable antennas, the impact on antenna characteristics in the vicinity of a human body has been investigated with a torso phantom. The torso (TORSO-OTA-V5.1 from SPEAG) is an anthropomorphically shaped [34] shell phantom which is filled with a broadband tissue simulating gel complying with human target parameters in [35], [36] up to 6 GHz. The antenna loaded with circularly polarized patch module is chosen in this study due to its high sensitivity in terms of circularly polarized antenna performance. The measured antenna reflection coefficient and axial ratio for the LHCP antenna placed on the phantom are plotted in Fig. 6 and Fig. 7 respectively. For representation of the radiation characteristics in Fig 8, the on-body radiation patterns are normalized to the maximum values in free space, and a slight reduction in LHCP component due to the torso phantom is observed in both planes. This is confirmed with the simulated and measured realized gain of the antenna shown in Fig. 14. In most of the frequency range, there is a reasonable agreement between the antenna realized gain measured in free space and with the phantom. Only a small gain decrement (maximum 0.7 dB) due to the human body is observed in a short frequency range around 5 GHz.

All these results indicate a rather low impact on the antenna performance when worn on the human body. The resilience to degradation when worn on the body is attributed to the isolation effect of the ground plane.

E. Bending Impact

Another critical aspect of wearable antennas is the influence of bending on their performance. To assess this effect, an investigation of the LHCP-patch-loaded antenna under two bending configurations has been carried out. The bending test setup is shown in the inset of Fig. 15: namely bending along the y-axis with radius of 30 mm (approximately a forearm radius) and 40 mm (approximately an upper arm radius)

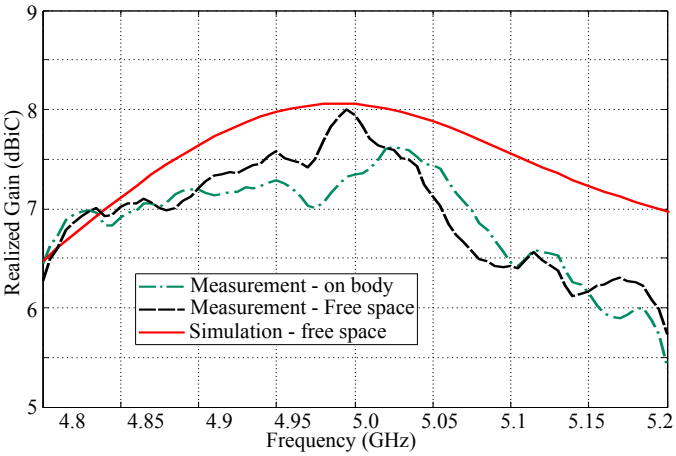

Figure 14. Simulated and measured realized gain of the LHCP antenna.

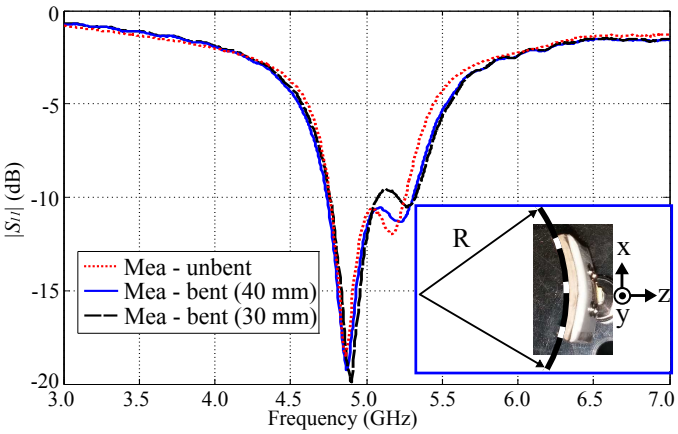

Figure 15. Measured reflection coefficients of the antenna under unbent and bent conditions. The inset shows the bending test settings. Two bending radii of the antenna have been determined as R = 30 mm and R = 40 mm respectively. The antenna was bent along the y-axis.

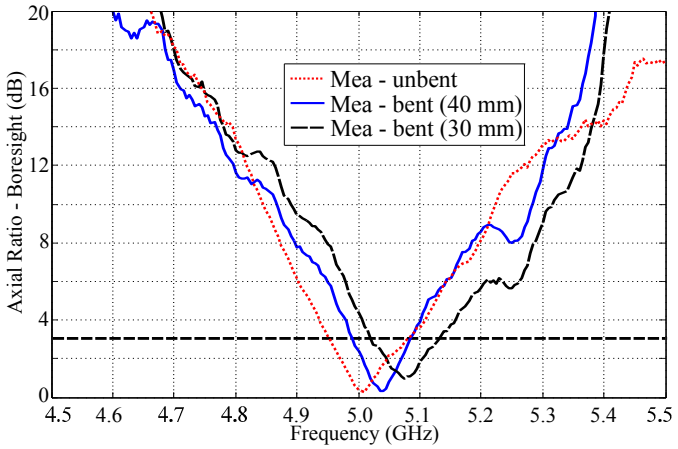

Figure 16. Measured axial ratios of the antenna under unbent and bent conditions.

respectively. Practically, bending along the x-axis should be avoided since more significant alterations in the effective patch length ($L2$) and consequently resonance frequency are anticipated [11], [37]. The measured reflection coefficients of the antenna under unbent and two bent configurations are illustrated in Fig. 15. There are no significant variations on the measured $|S_{11}|$ parameters introduced through the antenna bending. This is attributed to the compact size of the antenna leading to minor bending which results in only a small effective antenna length alteration. This result implies that the bending configuration should have a small influence on the impedance bandwidth of both circularly and linearly polarized modules.

In regards to the axial ratio of the bending antenna, the measured results are plotted in Fig. 16. According to the measurements, the axial ratio at 5 GHz is less than 3 dB and 5 dB for 40-mm and 30-mm bending radii, respectively. This degradation of the axial ratio bandwidth is not unexpected and can be caused by the changes in the resonance frequencies and the phase differences of both orthogonal modes [37]. A similar phenomenon for a bent circularly polarized textile antenna has been reported in [11]. These findings suggest that the axial ratio of the antenna is still within an acceptable range with a small bending radius (considering an often quoted relaxed tolerance of 6 dB). Therefore, the study indicates that the bending effect should still allow operation of the antenna with slightly degraded axial ratio.

IV. Conclusion

A modular antenna design for wearable applications has been proposed utilizing commercial snap-on buttons as mechanical and electrical (RF) connectors. Different textile patch modules can be designed to serve various functionalities such as variations in antenna resonance frequency, polarization and possibly beam direction. These modules can be attached to one common proximity-feeding base consisting of ground plane, substrate and open microstrip line. Therefore, this antenna design brings advantages such as low manufacture and maintenance cost, and most importantly, provides a passive way to reconfigure system characteristics for multi-functional wearable systems. Three modules providing interchangeability in circular polarization and resonance bands have been designed, manufactured and experimentally characterized. The measurement results are in very good agreement with simulations. The impact on antenna characteristics due to human body vicinity and small radius bending have also been investigated and the results indicate only an insignificant effect on the reflection coefficient, but some degradations of the circular polarization, which is notoriously sensitive to geometry variation. In addition, other potential patch modules offering interchangeable tilt beam direction and multi-band or wideband performance can be designed. All these findings indicate that, through utilizing modular design with a single feed, a wide range of functionalities can be fulfilled for various applications.

References

[1] I. Locher and G. Tröster, "Fundamental Building Blocks for Circuits on Textiles," *IEEE Trans. Adv. Packag.*, vol. 30, no. 3, pp. 541–550, Aug. 2007.

[2] N. H. M. Rais, P. J. Soh, F. Malek, S. Ahmad, N. Hashim, and P. Hall, "A review of wearable antenna," in *2009 Loughborough. Antennas Propag. Conf.*, 2009.

[3] P. S. Hall and Y. Hao, "Antennas and propagation for body centric communications," in *2006 First Eur. Conf. Antennas Propag.* IEEE, Nov. 2006, pp. 1–7.
[4] P. J. Soh, G. A. Vandenbosch, M. Mercuri, and D. M.-P. Schreurs, "Wearable Wireless Health Monitoring: Current Developments, Challenges, and Future Trends," *IEEE Microw. Mag.*, vol. 16, no. 4, pp. 55–70, 2015.
[5] K. Koski, A. Vena, L. Sydanheimo, L. Ukkonen, and Y. Rahmat-Samii, "Design and implementation of electro-textile ground planes for wearable UHF RFID patch tag antennas," *IEEE Antennas Wirel. Propag. Lett.*, vol. 12, pp. 964–967, 2013.
[6] A. Tsolis, W. Whittow, A. Alexandridis, and J. Vardaxoglou, "Embroidery and Related Manufacturing Techniques for Wearable Antennas: Challenges and Opportunities," *Electronics*, vol. 3, no. 2, pp. 314–338, 2014.
[7] C. Hertleer, A. Tronquo, H. Rogier, L. Vallozzi, and L. Van Langenhove, "Aperture-Coupled Patch Antenna for Integration Into Wearable Textile Systems," *IEEE Antennas Wirel. Propag. Lett.*, vol. 6, no. 11, pp. 392–395, 2007.
[8] L. Zhang, Z. Wang, and J. L. Volakis, "Textile Antennas and Sensors for Body-Worn Applications," *IEEE Antennas Wirel. Propag. Lett.*, vol. 11, pp. 1690–1693, 2012.
[9] C. Hertleer, A. Tronquo, H. Rogier, and L. Van Langenhove, "The Use of Textile Materials to Design Wearable Microstrip Patch Antennas," *Text. Res. J.*, vol. 78, no. 8, pp. 651–658, Aug. 2008.
[10] C. Hertleer, H. Rogier, L. Vallozzi, and L. Van Langenhove, "A Textile Antenna for Off-Body Communication Integrated Into Protective Clothing for Firefighters," *IEEE Trans. Antennas Propag.*, vol. 57, no. 4, pp. 919–925, Apr. 2009.
[11] E. K. Kaivanto, M. Berg, E. Salonen, and P. de Maagt, "Wearable Circularly Polarized Antenna for Personal Satellite Communication and Navigation," *IEEE Trans. Antennas Propag.*, vol. 59, no. 12, pp. 4490–4496, Dec. 2011.
[12] Z. Wang, L. Zhang, Y. Bayram, and J. L. Volakis, "Embroidered Conductive Fibers on Polymer Composite for Conformal Antennas," *IEEE Trans. Antennas Propag.*, vol. 60, no. 9, pp. 4141–4147, Sep. 2012.
[13] M. Klemm and G. Troester, "Textile UWB Antennas for Wireless Body Area Networks," *IEEE Trans. Antennas Propag.*, vol. 54, no. 11, pp. 3192–3197, Nov. 2006.
[14] P. B. Samal, P. J. Soh, and G. a. E. Vandenbosch, "UWB all-textile antenna with full ground plane for off-body WBAN communications," *IEEE Trans. Antennas Propag.*, vol. 62, no. 1, pp. 102–108, 2014.
[15] Q. H. Abbasi, M. U. Rehman, X. Yang, A. Alomainy, K. Qaraqe, and E. Serpedin, "Ultrawideband band-notched flexible antenna for wearable applications," *IEEE Antennas Wirel. Propag. Lett.*, vol. 12, pp. 1606–1609, 2013.
[16] R. Moro, S. Agneessens, H. Rogier, and M. Bozzi, "Wearable textile antenna in substrate integrated waveguide technology," *Electron. Lett.*, vol. 48, no. 16, pp. 985–987, Aug. 2012.
[17] T. Kaufmann and C. Fumeaux, "Wearable Textile Half-Mode Substrate-Integrated Cavity Antenna Using Embroidered Vias," *IEEE Antennas Wirel. Propag. Lett.*, vol. 12, pp. 805–808, 2013.
[18] S. Agneessens and H. Rogier, "Compact half diamond dual-band textile HMSIW on-body antenna," *IEEE Trans. Antennas Propag.*, vol. 62, no. 5, pp. 2374–2381, 2014.
[19] B. Sanz-Izquierdo, F. Huang, and J. Batchelor, "Covert dual-band wearable button antenna," *Electron. Lett.*, vol. 42, no. 12, p. 668, Nov. 2006.
[20] R. Garg, P. Bhartia, I. Bahl, and A. Ittipiboon, "Button Antenna on Textiles for Wireless Local Area Network On Body Applications," *IET Microwaves, Antennas Propag.*, vol. 4, no. May, pp. 1980–1987, 2010.
[21] T. Kellomäki, "Snaps to Connect Coaxial and Microstrip Lines in Wearable Systems," *Int. J. Antennas Propag.*, vol. 2012, pp. 1–10, 2012.
[22] B. Ivsic, D. Bonefacic, and J. Bartolic, "Considerations on Embroidered Textile Antennas for Wearable Applications," *IEEE Antennas Wirel. Propag. Lett.*, vol. 12, pp. 1708–1711, 2013.
[23] S. J. Chen, C. Fumeaux, D. C. Ranasinghe, and T. Kaufmann, "Paired Snap-On Buttons Connections for Balanced Antennas in Wearable Systems," *IEEE Antennas Wirel. Propag. Lett.*, vol. 14, no. X, pp. 1498–1501, 2015.
[24] K.-L. Wong and Z.-G. Liao, "Passive Reconfigurable Triple-Wideband Antenna for LTE Tablet Computer," *IEEE Trans. Antennas Propag.*, vol. 63, no. 3, pp. 901–908, 2015.
[25] D. J. Gioia, R. G. Uskali, and P. A. Kindinger, "Modular printed antenna," U.S. Patent 20 030 169 205 A1, Sep. 11, 2003.
[26] M. Johansson, S. Petersson, and S. Johansson, "Modular high-gain antennas," in *2008 IEEE Antennas Propag. Soc. Int. Symp.*, vol. 1, no. 1, Jul. 2008, pp. 1–4.
[27] G. Quagliaro, "Modular antenna system," U.S. Patent 6 831 610 B2, Dec. 14, 2004.
[28] C. C. Chen, "Beamforming structure for modular phased array antennas," U.S. Patent 5 162 803, Nov. 10, 1992.
[29] M. Lara, M. Mayes, W. Nunnally, T. Holt, and J. Mayes, "Modular interchangeable high power helical antennas," in *2011 IEEE Pulsed Power Conf.*, Jun. 2011, pp. 358–363.
[30] R. Garg, P. Bhartia, I. Bahl, and A. Ittipiboon, *Microstrip antenna design handbook*. Artech House, 2001.
[31] C. Balanis, *Antenna theory: analysis and design*, 2005.
[32] C. Hertleer, A. van Laere, H. Rogier, and L. van Langenhove, "Influence of relative humidity on textile antenna performance," *Text. Res. J.*, vol. 80, no. 2, pp. 177–183, 2010.
[33] R. Salvado, C. Loss, R. Gonçalves, and P. Pinho, "Textile materials for the design of wearable antennas: a survey," *Sensors.*, vol. 12, no. 11, pp. 15 841–57, Jan. 2012.
[34] C. C. Gordon, T. Churchill, C. E. Clauser, B. Bradtmiller, and J. T. McConville, "Anthropometric Survey of U.S. Army Personnel: Methods and Summary Statistics 1988," 1989.
[35] CTIA, "Test Plan for Wireless Device Over- the-Air Performance," 2013.
[36] G. TR25.914, "Measurements of radio performances for UMTS terminals in speech mode."
[37] T. Kellomäki, "Analysis of Circular Polarization of Cylindrically Bent Microstrip Antennas," *Int. J. Antennas Propag.*, vol. 2012, pp. 1–8, 2012.

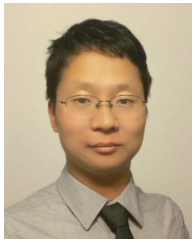

Shengjian Jammy Chen (S'13) received the B.S degree in information engineering from the Guangdong University of Technology, Guangzhou, China, in 2003, and the M.S degree in electrical and electronic engineering from the University of Adelaide, Adelaide, Australia, in 2013. He is currently working toward the Ph.D. degree in electrical and electronic engineering at the University of Adelaide. His current research interests include wearable and reconfigurable electromagnetic structures based on novel conductive materials such as conductive polymers and conductive fabrics, RFID-based wearable applications and leaky wave antennas.

He was the recipient of the Young Scientist Best Paper Award at the 2015 International Conference on Electromagnetics in Advanced Applications (ICEAA 2015).

Thomas Kaufmann (M'11) received his MSc degree in Electrical Engineering and Information Technology from ETH Zürich, Zürich, Switzerland, in 2007, and his PhD degree at the Laboratory for Electromagnetic Fields and Microwave Electronics (IFH), ETH Zürich in 2011. From 2011 to 2015, he was a lecturer and a postdoctoral researcher at the School of Electrical and Electronic Engineering at the University of Adelaide, Australia. In 2015, he joined SAFEmine (part of Hexagon Mining) in Baar, Switzerland as manager of the Advanced Technologies Group.

His research interests include wearable electromagnetic structures made from conductive polymers and fabrics, substrate-integrated antennas and computational electromagnetics in the microwave and THz region as well as UWB Ranging and Localization Technologies. He was the recipient of the best symposium paper award at the 2012 Asia-Pacific International Symposium on Electromagnetic Compatibility and 17ème Colloque International et Exposition sur la Compatibilité ÉlectroMagnétique 2014, and supervisor of a number of recipients of best paper awards at the International Workshop on Antennas and Propagation 2014 and 2014 Australian Microwave Symposium Best Student Paper Award. He has been serving as chair of the South Australian IEEE Joint AP/MTT Chapter from 2013 to 2015 and is a member of the EurAAP Working Group on Small Antennas.

Damith Chinthana Ranasinghe received his Ph.D. degree in electrical and electronic engineering from the University of Adelaide, Australia, in 2007. Since then, he has held an internship position at MIT in 2005 and a post-doctoral research position at the University of Cambridge from 2007–2009. He joined the University of Adelaide in 2010 and is currently a tenured Senior Lecturer at the School of Computer Science where he leads the research group at the Adelaide Auto-ID Lab. His research interests include pervasive and ubiquitous computing, wearable computing, human activity recognition, gerontechnology, and lightweight cryptography for resource constrained devices.

Christophe Fumeaux (M'03-SM'09) received the Diploma and Ph.D. degrees in physics from the ETH Zürich, Switzerland, in 1992 and 1997, respectively. From 1998 to 2000, he was a Postdoctoral Researcher with the School of Optics, University of Central Florida, Orlando. In 2000, he joined the Swiss Federal Office of Metrology, Bern, Switzerland, as a Scientific Staff Member. From 2001 to 2008, he was a Research Associate and Group Leader with the Laboratory for Electromagnetic Fields and Microwave Electronics, at ETH Zurich, Switzerland. Since 2008, he has been with The University of Adelaide, where he is currently a Professor with the School of Electrical and Electronic Engineering. His current main research interests concern computational electromagnetics, antenna engineering, THz technology and the application of RF design principles to optical micro/nano-structures.

Prof. Fumeaux has served as an Associate Editor for the IEEE Transactions on Microwave Theory and Techniques from 2010 to 2013. He serves currently as Associate Editor-in-Chief for the IEEE Transactions on Antennas and Propagation. He was the recipient of the ETH Silver Medal of Excellence for his doctoral dissertation. From 2011 to 2015, he was a Future Fellow of the Australian Research Council. He was the recipient/corecipient of best journal paper awards, including the 2004 ACES Journal and 2014 IEEE Sensors Journal, as well as best conference paper awards at the 2012 Asia-Pacific International Symposium on Electromagnetic Compatibility (APEMC 2012) and the 17th Colloque International sur la Compatibilité Electromagnétique (CEM 2014). Several of his students have received student awards with joint papers, including IMS 2006 & 2007, iWAT 2014, AMS 2014, IEEE Australia Council 2014, NEMO 2015, ICEAA 2015.